



Effects of annealing treatment on microstructure and hardness in the 28 wt% Cr cast iron with Mo/W addition

Kittikhun RUANGCHAI¹, Ruangdaj TONGSRI², John T. H. PEARCE³, Torranin CHAIRUANGSRI⁴, and Amporn WIENGMOON^{1,*}

¹ Department of Physics, Faculty of Science, Naresuan University, Phitsanulok, 65000, Thailand

² Powder Metallurgy Research and Development Unit (PM-RDU), Thailand National Metal and Materials Technology Center, Pathum Thani, 12120, Thailand

³ Panyapiwat Institute of Management, Nonthaburi 11120, Thailand

⁴ Department of Industrial Chemistry, Faculty of Science, Chiang Mai University, Chiang Mai 50200, Thailand

*Corresponding author e-mail: ampornw@nu.ac.th

Received date:

27 January 2021

Revised date

8 April 2021

Accepted date:

9 April 2021

Keywords:

High chromium cast iron;
Microstructure;
Annealing;
Hardness;
Carbide

Abstract

In this study, the effects of annealing on the hardness and microstructure of 28 wt% Cr-2.6 wt% C iron with 1.4 wt% Mo/1 wt% W addition have been investigated. The as-cast samples were heated to 800°C and held for 4 h followed by slow cooled with a cooling rate of 20°C·h⁻¹ to 500°C. Microstructures were characterized by X-ray diffractometry, optical microscopy, scanning electron microscopy and energy-dispersive X-ray spectroscopy. Vickers macro-hardness and micro-hardness were measured. It was found that the as-cast microstructure in the hypoeutectic 28 wt% Cr iron without Mo or W addition consisted of primary austenite dendrite, eutectic M₇C₃ carbide and martensite. In the iron with 1.4 wt% Mo addition, multiple eutectic carbides of M₇C₃, M₂₃C₆ and M₆C were observed. In contrast the addition of 1 wt% W changed the structure to hypereutectic containing primary M₇C₃, eutectic M₇C₃ and martensite. After the annealing heat treatment, ferrite +secondary carbides and some pearlite were present in the irons, due to decomposition of austenite during annealing. The macro-hardness in the as-cast condition of the iron without alloying and the irons with 1.4 wt% Mo/ 1 wt% W addition were 506, 529, and 576 HV₃₀, respectively. Annealing heat treatment reduced the macro-hardness to about 390, 463, and 428 HV₃₀, respectively.

1. Introduction

The most common materials used for abrasion resistant cast parts are high manganese steels, martensitic Ni-Cr white irons (Ni-Hard) and high chromium cast irons. High chromium cast irons (HCCIs) can bridge the toughness gap between the low toughness/ good abrasion resistance Ni-Hard irons and the higher toughness/ lower abrasion resistance high manganese steels [1,2]. HCCIs are widely used in industrial applications which need high hardness and wear resistance, for example tube mill liners and media in cement manufacturing, impact hammers, breaker bars, rollers, augers and shot blast parts. Irons consisting of 27 wt% to 30 wt% Cr and 2.0 wt% to 2.7 wt% C have been especially improved for combined abrasion and corrosion resistance in wet wear applications such as slurry pumping. The wear and fracture behavior of HCCIs depend on the type and proportion of hard eutectic carbides and on the nature of the matrix supporting the eutectic carbides. Heat treatment processes and alloying additions with carbide-forming elements such as V, Mo and W are used to improve wear resistance of these irons [1-7]. Normally, Mo is added to HCCI to control the transformation of austenite during cooling in the mold after casting, and during hardening and tempering heat treatments. Mo increases as-cast hardenability thus allowing

a pearlite-free austenite matrix when irons are to be used in the as-cast condition for parts such as liner plates and large slurry pump bodies [5-8]. W addition enhances the carbide volume fraction and promotes the formation of W-rich M₇C₃, M₆C and M₂₃C₆ that increase the hardness [6,8,9]. HCCI castings can be used for abrasion resistance without the need for machining.

However, there are some applications for which machining operations are necessary, such as crusher rollers and slurry pump bodies/side plates. These castings must have accurately machined fitting faces for assembly with other parts during fabrication or maintenance. HCCIs are difficult to machine due to the presence of hard eutectic carbides, hard martensitic matrices and work hardening of any austenite in the matrix. Cubic boron nitride (CBN) tools are needed to replace the conventional carbide or alumina ceramic tooling and to avoid grinding with silicon carbide wheels [11-13]. Grinding is a slow method and may also cause rapid local heating and grinding cracks, CBN cutting tool enable cost effective machining of austenitic matrices in as-cast irons or of tempered martensitic matrices in hardened irons. Annealing heat treatments in the temperature range of 700°C to 950°C can be used to decrease the hardness to below 400 HV at which machining is possible with conventional coated carbide tools [11-14]. During annealing, austenite can be transformed into a ferrite

matrix containing pearlitic and/or secondary carbides [11-15]. After annealing treatment and machining, the hardness and wear resistance of the irons can be improved by re-austenitization and destabilization following by air quenching to room temperature to form hard martensite matrices which can be subsequently tempered to reduce retained austenite levels and to improve toughness.

Agunsoye *et al.* [16] found that, after annealing 22 wt% Cr-2.9 wt% C iron in a muffle furnace at 750°C for 2 h, and then furnace cooling, the as-cast and annealed hardness values were 590 HB and 428 HB, respectively. Berkun *et al.* [17] suggested that, to improve machinability, 27 wt% Cr-2.5 wt% C iron should be annealed in the temperature range of 800°C to 900°C, which can reduce the hardness to 320 HV to 350 HV, because of the decomposition of austenite to ferrite and secondary carbide. Kibble and Pearce [11] found that the microstructure of 25 wt% Cr-2.5 wt% C iron consisted of a fully ferrite matrix with secondary carbides after annealing at 950°C and holding for 4 h, followed by a slow cool of 20°C·h⁻¹. Whereas, after annealing at 750°C, some pearlite was formed in the central zones of the dendrites in the matrix with coarse secondary carbides at the edges. The hardness levels after annealing at 750°C and 950°C were 370 HV and 349 HV, respectively. Furthermore, addition 0.77 wt% Mo to the 25 wt% Cr iron gave a microstructure containing more pearlite with finer carbides within the ferrite matrix increasing the hardness up to 413 HV and 388 HV, respectively. Chen *et al.* [13] reported the microstructure and hardness of the 25 wt% Cr-2.7 wt% C-0.8 wt% Si iron after an annealing treatment that involved four steps: heating to 930°C holding for 1.5 h, cooling to 650°C holding for 1 h, cooling to 600°C holding time for 2 h and then cooling to room temperature. It was found that after annealing the matrix transformed mainly to bainite with secondary carbides. The as-cast and annealed hardness were 580 HV and 330 HV, respectively. In addition to reducing the hardness of irons for machining with conventional tools, prior-annealing has been used for homogenizing before destabilization [15-17]. Cubillos *et al.* [14] studied the effect of prior-annealing on destabilized hardness and wear resistance of the 22 wt% Cr-3 wt% C iron. It was found that destabilization time required to achieve high hardness and satisfactory wear resistance could be reduced by prior-annealing.

Generally, the microstructure and annealed hardness depend on the annealing temperature and time, the cooling cycle and rate, and the presence of alloying elements. Mo and W additions to HCCIs are important alloying element for used in applications as mention earlier. It was found that Mo addition increased the annealed hardness to about 413 HV [11]. However, the effects of W addition on the annealed hardness had less information. Our previous work [18] found that

the hardness of 28 wt% Cr-2.6 wt% C cast iron was 425 HV30 after annealing at 800°C for 4 h, followed by a furnace cool of 40°C·h⁻¹. In the present study, therefore, the effects of three steps annealing heat treatment with a slow cool of 20°C·h⁻¹ on the microstructures and hardness of 28 wt% Cr-2.6 wt% C iron with Mo and W additions have been further investigated.

2. Experimental

All the irons in this work were prepared by melting in a magnesia crucible, using an electric resistance furnace. The irons were cast into dry sand molds as cylindrical test bars with 25 mm in diameter × 300 mm in length. Table 1 shows nominal compositions of the irons. In this study, the as-cast samples were heated to 800°C and held for 4 h, followed by slow cooling at 20°C·h⁻¹ to 500°C, and then furnace cooled to room temperature. The annealing process cycle is shown in Figure 1.

For the microstructural investigation, the samples were prepared by grinding on silicon carbide papers and then polishing with 6, 3, 1 μm diamond paste. Two etchants were used for etching: (i) 50 mL of HCl and 10 g of Na₂S₂O₅ in 100 mL distilled water, and (ii) 10 vol% HCl in methanol for deep etching. The microstructural characteristics and phase identification were analyzed using X-ray diffraction technique (XRD), optical microscopy (OM), scanning electron microscopy (SEM) and energy-dispersive X-ray spectroscopy (EDS). The volume fraction of total carbides was measured by ImageJ software, the average value was based on eight different areas.

Vickers macro-hardness testing was performed on polished specimens using 30 kgf load (HV30) at 15 s indentation time. Vickers micro-hardness testing was also performed on the matrix areas of etched specimens using 100 gf load (HV0.1) at 15 s indentation time, the average value was based on ten different areas.

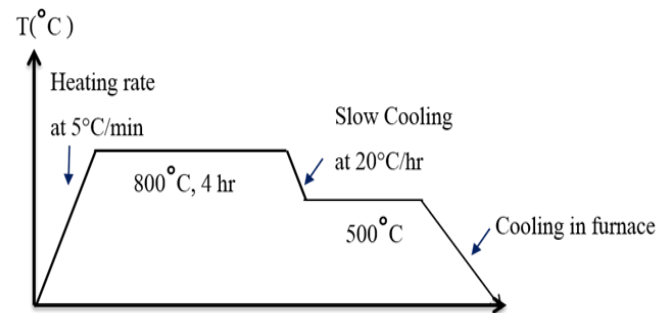


Figure 1. Annealing process in this experiment.

Table 1. Nominal composition of the irons used in this work.

Samples	Nominal composition (wt%)									
	C	Cr	W	Mo	Si	S	Ni	P	Mn	Fe
Ref.	2.36	27.86	0.01	0.20	0.20	0.01	0.20	0.02	0.11	Bal.
Mo1	2.68	27.65	0.01	1.42	0.26	0.01	0.2	0.02	0.11	Bal.
W1	2.87	26.67	0.99	0.03	0.44	0.01	0.22	0.03	0.15	Bal.

3. Results and discussion

3.1 As-cast microstructure

XRD analysis, as illustrated in Figure 2, revealed that the as-cast reference iron (R), Mo addition iron (Mo1) and W addition iron (W1) contained austenite, martensite and M_7C_3 carbide (M = Fe, Cr, Mo, W). Mo addition to 28 wt% Cr-2.6 wt% C iron promoted the formation of M_6C carbide. OM and SEM observations, as shown in Figure 3(a) and 3(b), confirmed that the as-cast microstructure of reference iron (R) consisted of primary austenite dendrites with eutectic M_7C_3 carbides and eutectic austenite which had partly transformed to martensite during cooling in the mold. As shown in Figure 3(c) and 3(d), multiple eutectic carbides including M_7C_3 , $M_{23}C_6$ and M_6C were found in the Mo1 iron. The three carbides, M_7C_3 , $M_{23}C_6$ and M_6C , were clearly distinguished via sequential, bright contrast in SEM-BEI because of differences in Mo content. Addition of 1 wt% W to 28 wt% Cr-2.6 wt% C iron changed the microstructure from hypoeutectic to hypereutectic resulting in the presence of primary M_7C_3 carbide with eutectic austenite and eutectic carbide ($\gamma + M_7C_3$) as illustrated in Figure 3(e) and 3(f). W addition moved the chemical composition towards hypereutectic, even at a relatively low content of 1 wt% W. The observation of primary M_7C_3 carbide agrees with the previous investigations by Anijdan *et al.* [8] and Imurai *et al.* [7,9]. The solidification sequence of the Mo1 and W1 irons can be outlined as: $L_0 \rightarrow$ primary $\gamma + L_1$, $L_1 \rightarrow$ eutectic ($\gamma + M_7C_3/M_{23}C_6/M_6C$) and $L_0 \rightarrow$ primary $M_7C_3 + L_1$, $L_1 \rightarrow$ eutectic ($\gamma + M_7C_3$), respectively.

SEM-EDS analysis of the reference iron (R) found that Fe is mainly dispersed in the austenite matrix, whereas the eutectic M_7C_3 carbide had high dispersion of Cr and C as expressed in Figure 4. When Mo is present in Mo1, it dissolves in both the matrix and carbides, as seen in Figure 5. Furthermore, Mo tends to segregate

to eutectic M_6C carbide, while the M_7C_3 and $M_{23}C_6$ carbides have high Cr content confirming that the brightest BSE contrast carbides with high Mo content were M_6C . Imurai *et al.* [7] reported that segregation of Mo during solidification could result in multiple eutectic $M_7C_3/M_{23}C_6/M_6C$ and that carbide transitions of the form $M_7C_3/M_{23}C_6/M_6C$ also increased with increasing Mo content.

The dispersion of W in the matrix, and in the primary and eutectic M_7C_3 carbides is shown in Figure 6. The 1 wt% W addition to 28 wt% Cr-2.6 wt% C iron increased the volume fraction of carbides from 36 vol% in the reference iron (R) up to 40 vol%, as shown in Figure 7, due to the formation of primary M_7C_3 carbide. However, 1.4 wt% Mo addition decreased the volume fraction of total carbides to about 33 vol% which is slightly lower than the reference iron (R). This may be due to the formation of M_6C and $M_{23}C_6$ carbides.

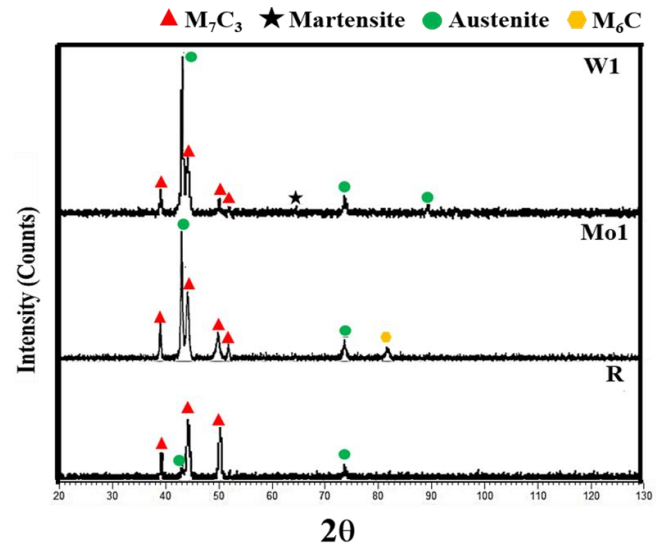


Figure 2. XRD patterns of reference iron (R), Mo1 and W1 irons in the as-cast condition.

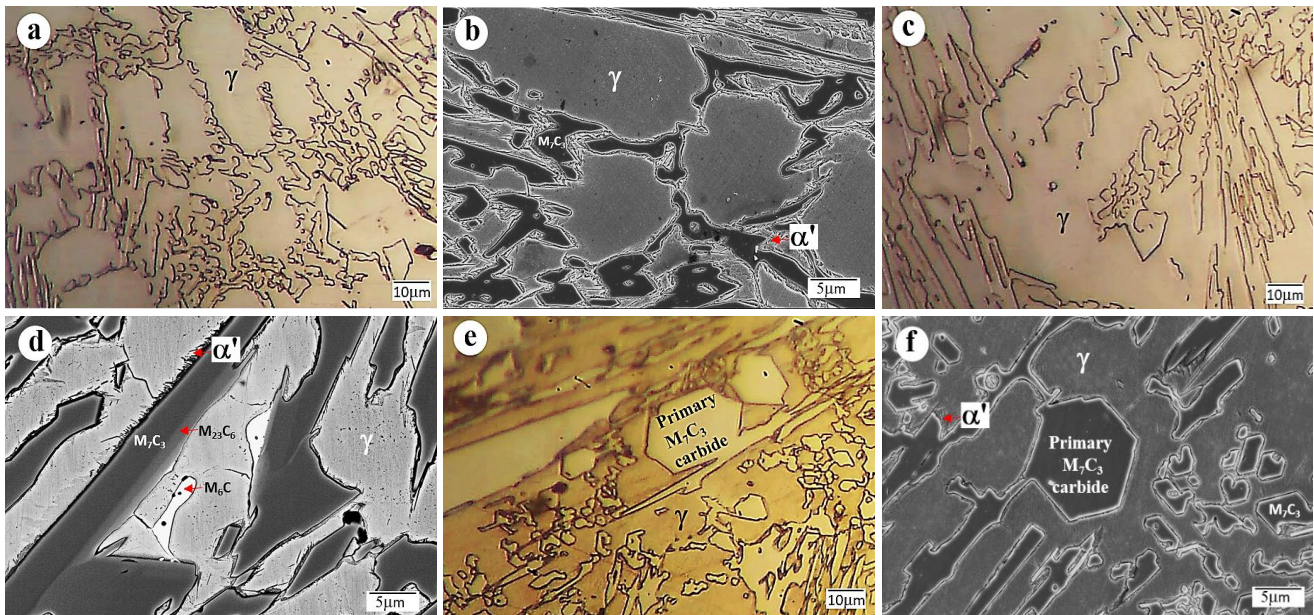


Figure 3. Optical micrographs and backscattered electron images (BEIs) show the as-cast microstructure of the irons (a, b) reference iron (R), (c, d) Mo1 iron (e, f) W1 iron.

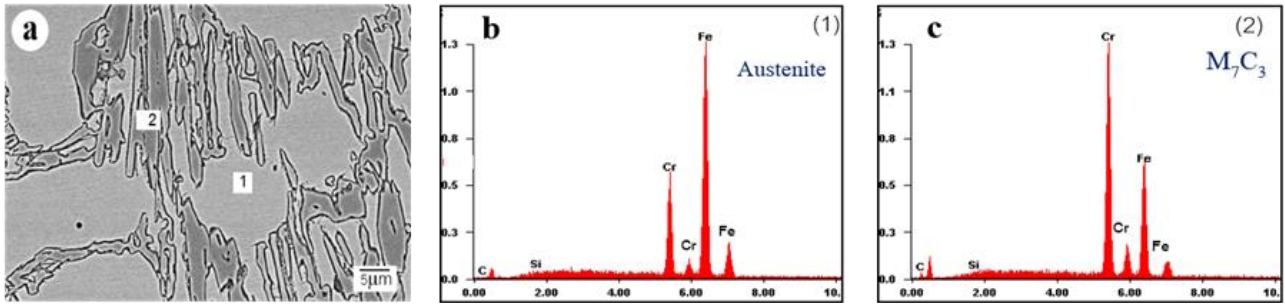


Figure 4. (a) SEM-BEI shows the microstructure in the reference iron (R) and (b-c) EDS spectra from the austenite matrix (1) and M_7C_3 carbide (2), respectively.

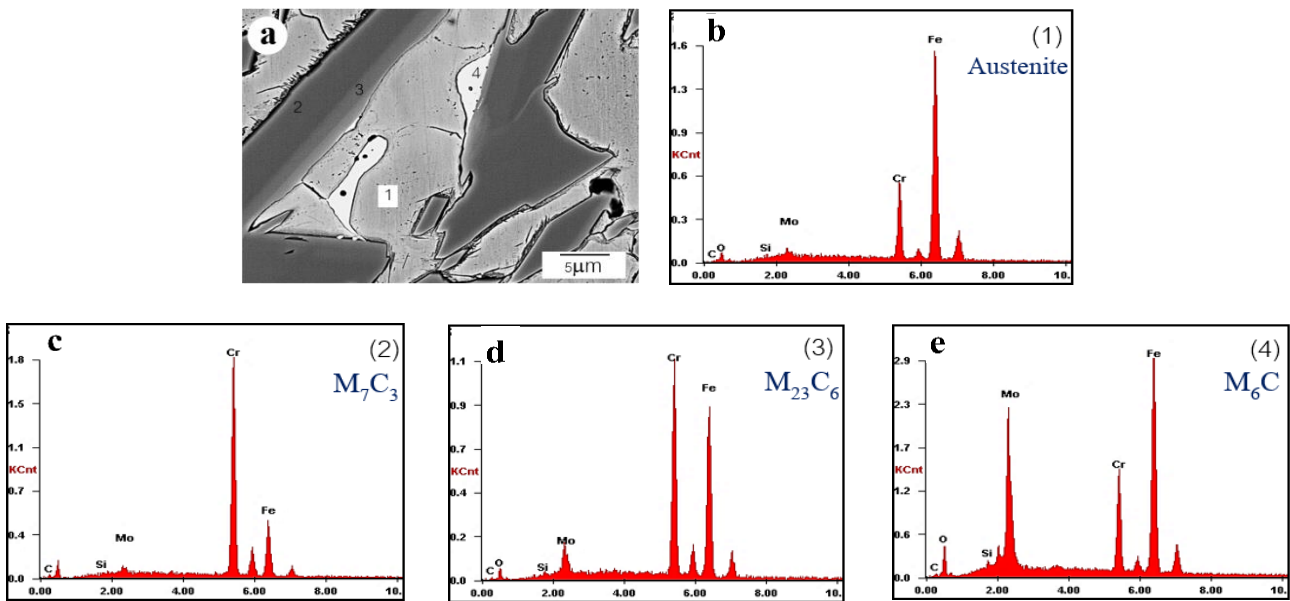


Figure 5. (a) SEM-BEI shows the multiple eutectic carbides in Mo1 iron (b-e) EDS spectra from the austenite matrix (1), M_7C_3 (2), $M_{23}C_6$ (3) and M_6C (4), respectively.

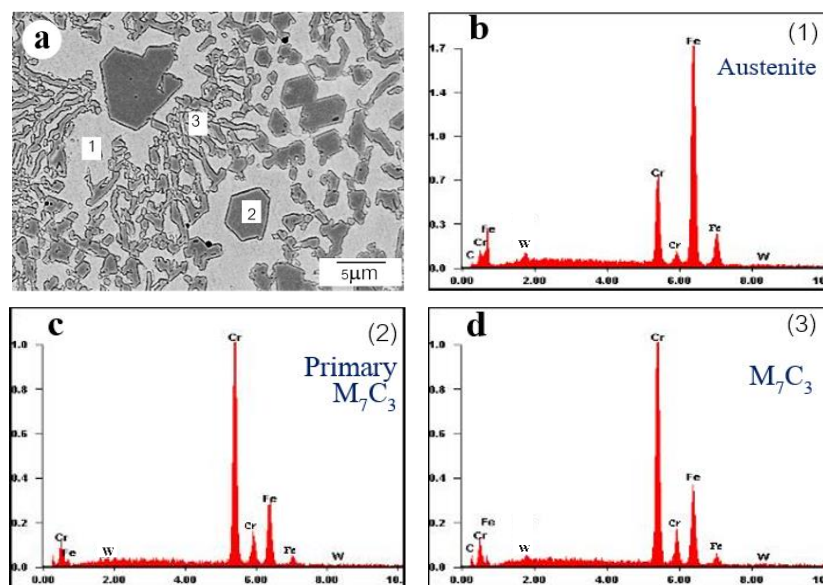


Figure 6. (a) SEM-BEI shows the hypereutectic structure in W1 iron (b-d) EDS spectra from the austenite matrix (1), primary M_7C_3 (2) and eutectic M_7C_3 (3), respectively.

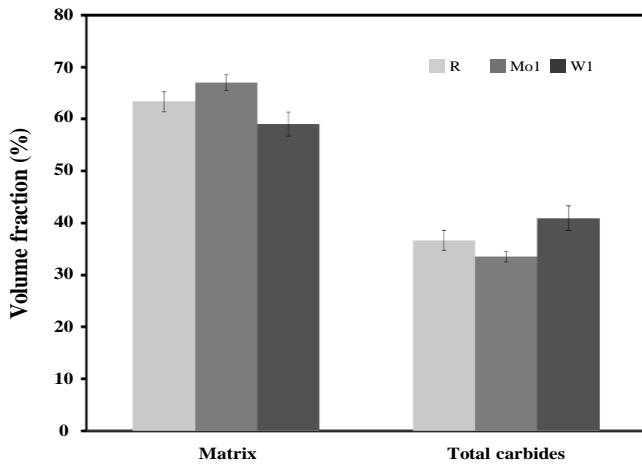


Figure 7. The effect of Mo and W addition on the volume fraction of matrix and total carbides of the reference iron (R), Mo1 and W1 irons.

3.2 Microstructure after annealing

XRD patterns in Figure 8 revealed the presence of ferrite, M_7C_3 and $M_{23}C_6$ in the reference iron (R), Mo1 and W1 iron after annealing. M_6C carbide was also found in the Mo1 iron. While M_3C (cementite) peaks were presented in the W1 iron. From OM and SEM observations, as shown in Figure 9, the microstructure of reference iron (R) after annealing consisted of a ferrite (α) matrix and secondary carbides within the matrix, due to decomposition of austenite during annealing [11,12,14,15]. Small areas of pearlite were also found in the central regions of the dendrite arms. Kibble and Pearce [11,12] suggested that the presence of small areas of pearlite meant that the transformation of austenite to ferrite and secondary carbides was incomplete because of microsegregation effects. The presence of M_3C peaks in XRD patterns

confirmed the transformation of austenite to pearlite during slow cooling annealing. The Mo1 and W1 irons also contained pearlite but it was finer compared to that in the reference iron (R).

Deep etching revealed the secondary carbides precipitation formed when during austenite transformation. As seen in Figure 10, the secondary carbides in the form of cube, discrete-rod or plate-like shapes tend to connect together to form a network, XRD suggests that the secondary carbides formed during annealing are $M_{23}C_6$. The Mo1 iron showed finer and denser secondary carbides compared with the reference iron (R) and W1 iron. Mo content in the matrix is known to promote the formation of fine secondary carbides [11-15].

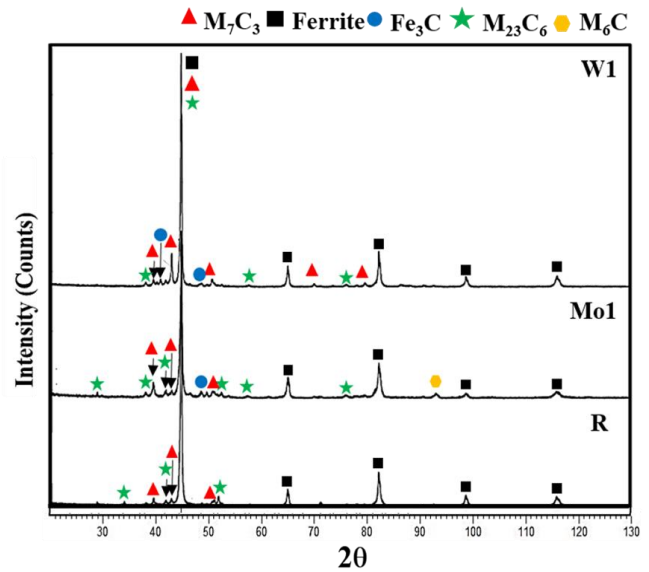


Figure 8. XRD patterns after annealing treatment of the reference iron (R), Mo1 and W1 irons.

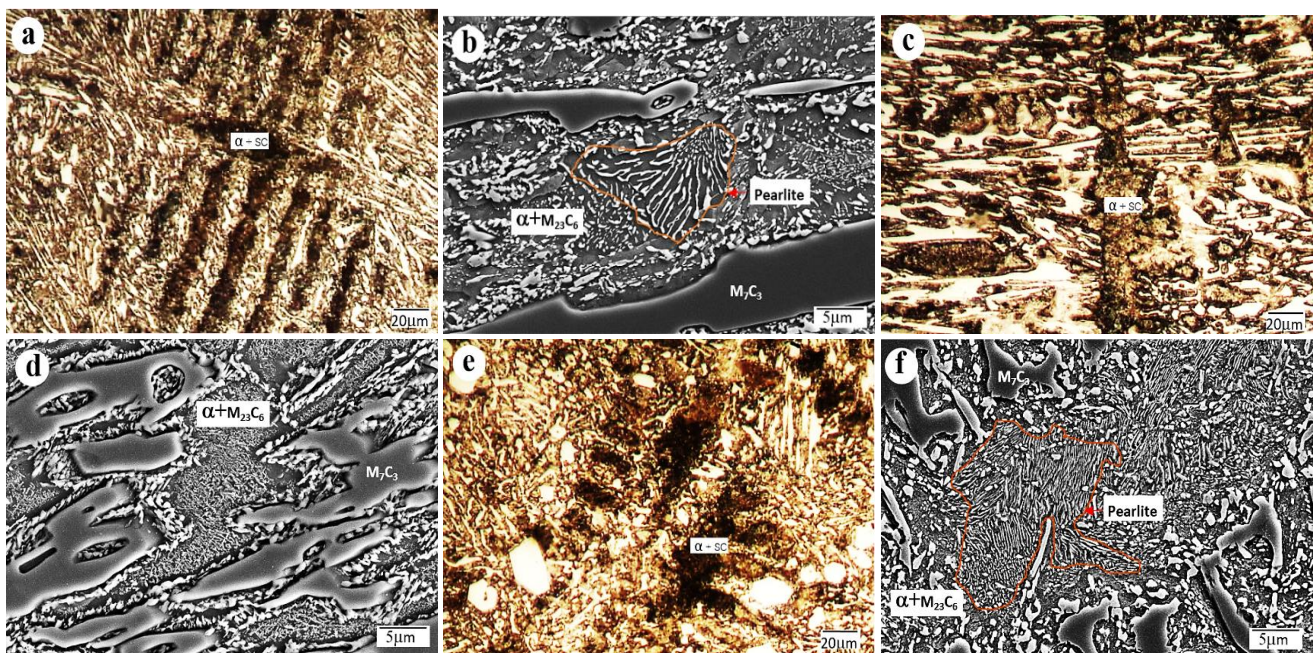


Figure 9. Optical micrographs and SEIs show the microstructure of the irons after annealing (a-b) reference iron (R), (c-d) Mo1 iron (e-f) W1 iron.

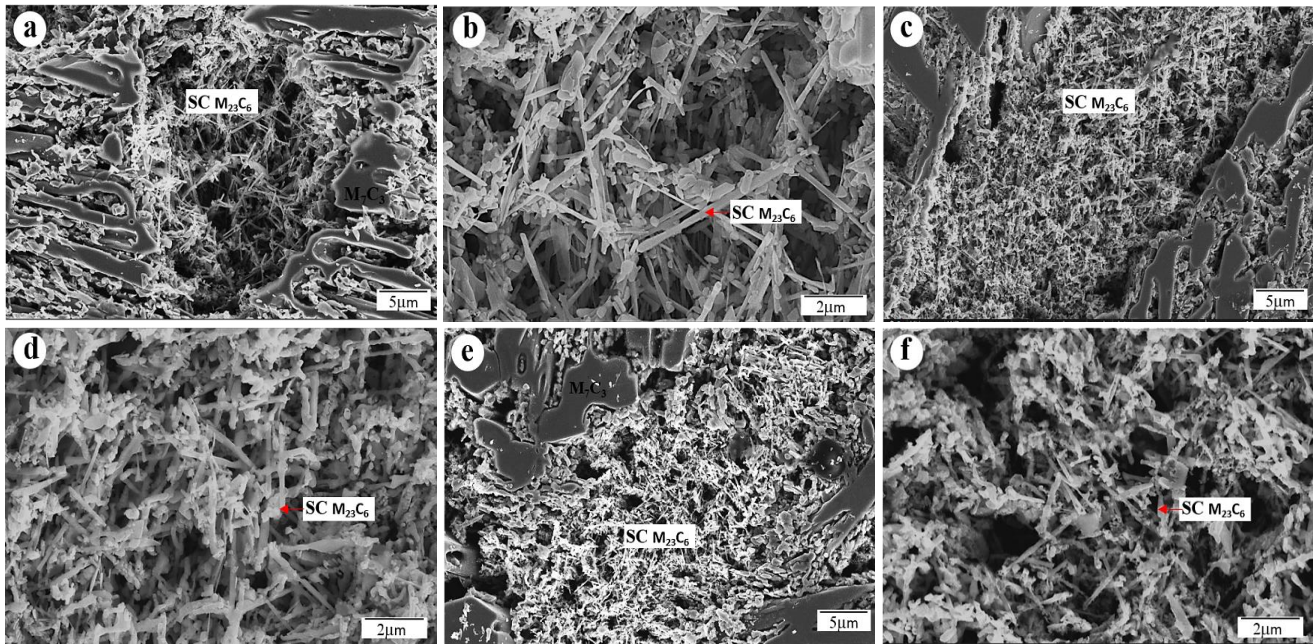


Figure 10. SEIs show deep etched structure of secondary carbides precipitated within ferrite matrix after annealing: (a-b) reference iron (R), (c-d) Mo1 iron (e-f) W1 iron.

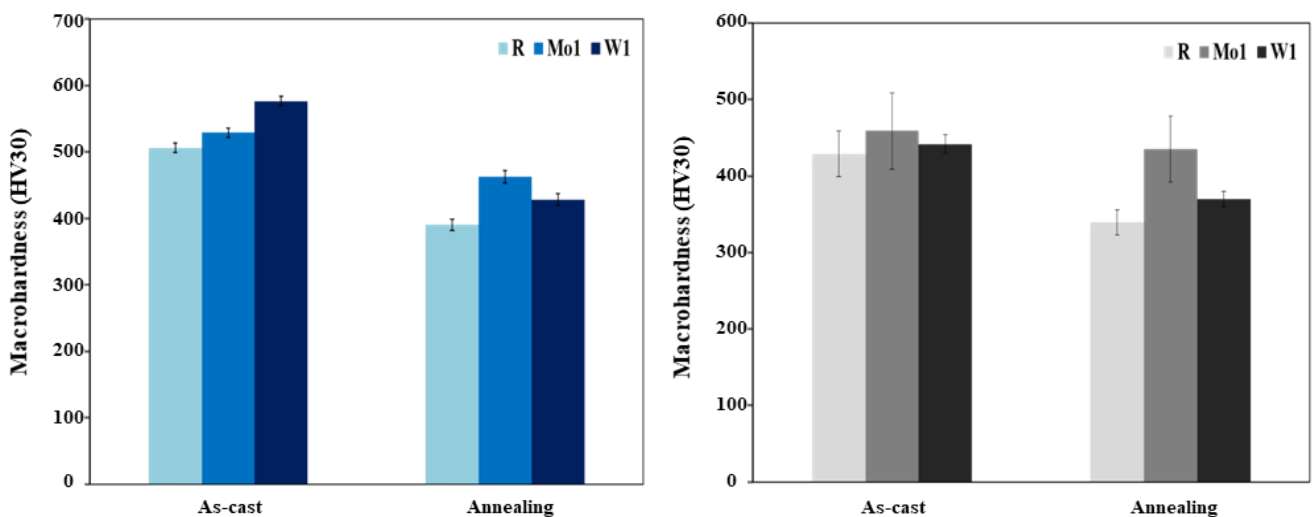


Figure 11. Effect of annealing and alloying on macro-hardness and micro-hardness (a) macro-hardness (b) micro-hardness.

3.3 Macro-hardness and Micro-hardness

Figure 11 compares the Vickers macro-hardness and micro-hardness in the as-cast condition and after annealing. It was found that the macro-hardness in the as-cast condition of the reference iron (R), Mo1 and W1 irons were 506, 529 and 576 HV30, and that the micro-hardness within the matrix regions were 429, 459, and 442 HV0.1, respectively. Addition of Mo increased the macro-hardness, due to the formation of M_6C carbide. The highest macro-hardness was obtained in the W1 iron due to the formation of primary M_7C_3 carbide and the high carbide volume fraction. However, Mo1 iron had higher micro-hardness than the reference iron (R) and

W1 iron which may be due to high Mo content as solid-solution in the matrix.

After annealing, the macro-hardness of the reference iron (R), Mo1 and W1 iron decreased from the as-cast condition to 390, 463, 428 HV30, and the micro-hardness to 339, 435, 370 HV0.1, respectively. This is due to the transformation of the austenite matrix to ferrite. Annealing heat treatment after holding at 800°C for 4 h, followed by a slow cooling at 20°C·h⁻¹, did not reduce the hardness below 400 HV in the Mo and W containing irons. The highest annealed hardness was obtained in the Mo1 iron. The finer secondary carbide precipitation with fine pearlite and formation M_6C are thought to be the main reasons for annealed hardness increase.

4. Conclusions

4.1 The as-cast microstructure of hypoeutectic 28 wt% Cr-2.6 wt% C iron consisted of primary austenite dendrite with eutectic M_7C_3 and eutectic austenite which had partly transformed to martensite during cooling. In the iron with 1.4 wt% Mo, multiple eutectic carbides of M_7C_3 , $M_{23}C_6$ and M_6C were observed. However, the volume fraction of total carbide decreased.

4.2 The iron with 1 wt% W addition was hypereutectic containing primary M_7C_3 , eutectic M_7C_3 carbides austenite and martensite. Addition of W also increased the volume fraction of total carbides.

4.3 After annealing, the matrix in all irons was ferrite plus secondary $M_{23}C_6$ carbide and some areas of pearlite. Addition of Mo and W to the 28 wt% Cr-2.6 wt% C iron gave finer and denser secondary carbides in annealed matrix with fine pearlite.

4.4 Annealing treatment at 800°C followed by a slow cooling at 20°C·h⁻¹ reduced the macro-hardness of the 28 wt% Cr-2.6 wt% C iron from 506 HV30 in the as-cast condition to about 390 HV30. However, via this treatment it is difficult to reduce the hardness in the irons with 1.4 wt% Mo/1 wt% W addition below 400 HV. This is due to the formation of fine secondary carbide, M_6C and primary M_7C_3 carbides.

Acknowledgements

The authors are grateful for financial and technical supports from Thailand Graduate Institute of Science and Technology: TGIST (TG-MT-NU-62-020D), Thailand National Metal and Materials Technology Center (MTEC) and Naresuan University (R2563C016).

References

- [1] C. P. Tabrett, I. R. Sare, and M. R. Ghomashchi, "Microstructure-property relationships in high chromium white iron alloys," *International Materials Reviews*, vol. 41, pp. 59-82, 1996.
- [2] G. Laird, R. Gundlach, and K. Rohrig, *Abrasion-resistant cast iron Handbook*. USA: AFS, 2000.
- [3] A. Wiengmoon, T. Chairuangri, A. Brown, R. Brydson, D. V. Edmonds, and J. T. H. Pearce, "Microstructural and crystallographical study of carbides in 30 wt%Cr cast irons," *Acta Materialia*, vol. 53, pp. 4143-4154, 2005.
- [4] M. Filipovic, Z. Kamberovic, and M. Korac, "Solidification of High Chromium white cast iron alloyed with vanadium," *Materials Transactions*, vol. 52, pp. 386-390, 2011.
- [5] P. Dupin, and J. M. Schissler, "Influence of addition of silicon, molybdenum, vanadium, and tungsten upon the structural evolution of the as-cast state of a high-chromium cast iron (20% Cr, 2.6% C)." *AFS Transactions*, vol. 92, pp. 355-360, 1984.
- [6] J. W. Choi, and S. K. Chang, "Effects of molybdenum and copper additions on microstructure of high chromium cast iron rolls." *ISIJ International*, vol. 32, pp. 1170-1176, 1992.
- [7] K. Yamamoto, S. Inthidech, N. Sasaguri, and Y. Matsubara, "Influence of Mo and W on high temperature hardness of M_7C_3 carbide in high chromium white cast iron," *Materials Transactions*, vol. 55, pp. 684-689, 2014.
- [8] S. Imurai, C. Thanachayanont, J. T. H. Pearce, K. Tsuda, and T. Chairuangri, "Effects of Mo on microstructure of as-cast 28 wt% Cr-2.6 wt% C-(0-10) wt% Mo irons." *Materials Characterization*, vol. 90, pp. 99-112, 2014.
- [9] S. H. Mousavi Anijdan, A. Bahrami, N. Varahram, and P. Davamic, "Effects of tungsten on erosion-corrosion behavior of high chromium white cast iron." *Materials Science and Engineering*, vol. 454-455, pp. 623-628, 2007.
- [10] S. Imurai, C. Thanachayanont, J. T. H. Pearce, K. Tsuda, and T. Chairuangri, "Effects of W on microstructure of as-cast 28 wt% Cr-2.6 wt% C-(0-10) wt% W irons." *Materials Characterization*, vol. 99, pp. 52-60, 2015.
- [11] K. A. Kibble, and J. T. H. Pearce, "An examination of the effects of heat treatment secondary carbide formation in 25% Cr high chromium irons," *Cast Metals*, vol. 8, pp. 123-127, 1995.
- [12] K. A. Kibble, and J. T. H. Pearce, "Influence of heat treatment on the microstructure and hardness of 19% high-chromium cast irons," *Cast Metals*, vol. 6, pp. 9-15, 1993.
- [13] L. Chen, J. Zhou, V. Bushlya, and J. E. Stahl, "Influences of micro mechanical property and microstructure on performance of machining high chromium white cast iron with CBN tools" *Procedia CIRP*, vol. 31, pp. 172-178, 2015.
- [14] P. O. Cubillos, P. A. N. Bernardini, M. C. Fredel, and R. A. Campos, "Wear resistance of high chromium white cast iron for coal grinding rolls," *Revista Facultad de Ingenieria, University of Antioquia*, vol. 76, pp. 134-142, 2015.
- [15] A. E. Karantzalis, A. Lekatou, and H. Mavros, "Microstructural modifications of as-cast high-chromium white iron by heat treatment," *Journal of Materials Engineering and Performance*, vol. 18, pp. 174-181, 2009.
- [16] J. O. Agunsoye, and A. A. Ayeni, "Effect of heat treatment on the abrasive wear behavior of high chromium iron under dry sliding condition." *Tribology in Industry*, vol. 34(2), pp. 82-91, 2012.
- [17] M. N. Berkun, I. P. Volchok, I. V. Zhivitsa, and V. I. Topal, "Effect of heat treatment on the properties of high-chromium cast iron." *Metal Science and Heat Treatment*, vol. 13, pp. 69-71, 1971.
- [18] A. Wiengmoon, J. Khantee, J. T. H. Pearce, and T. Chairuangri, "Effect of pre-annealing heat treatment on destabilization behavior of 28 wt% Cr-2.6 wt% C high-chromium cast iron, IOP Conference Series: Materials Science and Engineering, vol. 474, pp. 1-6, 2019.